

P10.3 HAIL DETECTION USING A POLARIMETRIC ALGORITHM AT C BAND: IMPACT ON ATTENUATION CORRECTION

Gianfranco Vulpiani¹, Pierre Tabary¹, Jacques Parent-du-Chatelet¹, Olivier Bouquet¹, M.-L. Segond¹, and Frank S. Marzano²

¹Meteo-France, DSO, Centre de Météorologie Radar, Trappes, France

²Dept. of Electronic Engineering, University La Sapienza, Rome, Italy

1. INTRODUCTION

Discrimination between rain and hail radar echoes is a long-standing objective for meteorological, aviation and agricultural applications. Hail detection using single polarized radar began in the late 1950s with techniques based on reflectivity measurements (Cook, 1958). A refinement of the relationship between the 45-dBZ level above the freezing level and the occurrence of hail at ground (Waldvogel et al., 1979) is currently used by the Weather Surveillance Radar-1988 Doppler (WSR-88D) systems. With the development of radar polarimetry the differential reflectivity Z_{dr} became the key radar parameter for hail detection (Seliga et al., 1982; Bringi et al., 1984). Since the late 1990s, fully polarimetric algorithms based on the Fuzzy Logic have been proposed for S-band weather radar classification of hydrometeors (Vivekanandan et al. 1999; Zrnić et al., 2001). Recent studies have confirmed the higher performance of Fuzzy Logic algorithms with respect to methodologies employing radar reflectivity only for the diagnosis of hail using radar measurements at S band (Heinselman and Ryzhkov, 2006).

The common underlying hypothesis of dual polarization methods is the isotropic radar appearance of hail even if it is oblate. The tumbling and gyrating motions confer a spherical-like behavior of hail (Knight and Knight, 1970), the corresponding Z_{dr} signature being near to zero. Based on disdrometer observations, Zrnić et al. (1993) assumed that both large oblate and prolate hailstones tend to fall with the minor axis in the horizontal producing negative values of Z_{dr} . Observations of oblate hailstones with the major axis in the horizontal are also documented in the literature (Smyth et al., 1998). Consequently, the fall mode, determined by Liquid Water Content (LWC) and updraft speed, is a crucial factor affecting the interpretation of polarimetric radar signatures and the set up of hail detection algorithms.

Nearly all European weather radars operate at C band. At frequencies higher than S band, path attenuation effects due to rainfall can be significant and need to be compensated for quantitative applications (Vulpiani et al., 2005). Hydrometeor classification at C band is a recent field of investigation (Alberoni et al., 2002; Marzano et al., 2007), whereas robust polarimetric algorithms for rain path attenuation are available (Bringi et al., 1990; Testud et al., 2000). Nevertheless, mixed precipitation may cause large attenuation that traditional methodologies are not able to deal with.

In a recent study Vulpiani et al. (2006) found anomalously high differential attenuation generated by cells characterized by high values of reflectivity, differential reflectivity, differential phase shift and low correlation coefficient. These observed polarimetric signatures seem to suggest the presence of rain mixed with horizontally oriented wet hail. During an intense squall line system observed in Germany with a C-band polarimetric radar, large values of differential reflectivity (6-8 dB) have been also observed in convective precipitation shaft (Meischner et al., 1991).

In this work, we explore a new hydrometeor classification-based iterative approach for attenuation and differential attenuation compensation. The preliminary discrimination between rain and rain mixed with wet hail enables the use of adaptive relationships between specific attenuation and specific differential phase. The classification algorithm represents the fully polarimetric version of the fuzzy-logic based approach proposed for C band by Marzano et al. (2007). An extreme convective storm observed during 2005 in the Paris area by the C-band dual-polarized weather radar operating in Trappes (Gourley et al., 2006a) is analyzed. The use of the proposed methodology sensibly reduces the observed path attenuation and differential attenuation which can reach values up to about 20 dBZ and 10 dB, respectively.

2. PATH ATTENUATION CORRECTION AND HAIL DETECTION

As found by Bringi et al. (1990), co-polar specific attenuation (α_{hh}) and differential attenuation (α_{dp}) are almost linearly related to specific differential phase (K_{dp}) in rain. In a recent study (Vulpiani et al., 2006), the authors exploited the adaptive use of differential phase (APDP) for rain path attenuation correction through a preliminary classification of the prevailing rain type by resorting to the Bayesian inference theory.

In the following paragraphs we will briefly illustrate the main concepts of the APDP approach and its improved version developed for the present study.

2.1 APDP APPROACH

The classification step, following a basic attenuation correction of reflectivity and differential reflectivity, guarantees the optimization of the proportionality coefficient $\gamma_{hh,dp}$ used for the cumulative attenuation A_{hh} [dB] estimation:

* Corresponding author address: Gianfranco Vulpiani, Centre de Météorologie Radar, DSO, Météo France, 7 rue Teisserenc-de-Bort 78195, Trappes, France; email: gianfranco.vulpiani@meteo.fr

$$A_{hh}(r) = \int_{r_0}^r \alpha_{hh}(s) ds = \gamma_{hh} \int_{r_0}^r K_{dp}(s) ds = \frac{\gamma_{hh}}{2} [\Phi_{dp}(r) - \Phi_{dp}(r_0)] = \frac{\gamma_{hh}}{2} \Delta \Phi_{dp}(r, r_0) \quad (1)$$

Following (1), the corrected reflectivity can be written as

$$10 \log_{10} [Z_{hh}(r)] = 10 \log_{10} [Z'_{hh}(r)] + 2A_{hh}(r) = 10 \log_{10} [Z'_{hh}(r)] + \gamma_{hh} \Delta \Phi_{dp}(r, r_0) \quad (2)$$

Equations analogous to (1) and (2) can be derived for A_{dp} and Z_{dr} , respectively.

As documented in the literature (Jameson, 1992), $\gamma_{hh,dp}$ depends on the raindrop size, shape and temperature. Consequently, a preliminary rain type classification enables the computation, at each range gate (r), of an average $\langle \gamma_{hh,dp} \rangle$ which correctly accounts for the different extinction properties of the rain type identified along the wave propagation path. In order to properly weight the single values of $\gamma_{hh,dp}(r)$ according to their contribution to the path attenuation, the following K_{dp} -weighted average of $\gamma_{hh,dp}$ is used in (2)

$$\langle \gamma_{hh,dp} \rangle_{K_{dp}} = \frac{\int_{r_0}^r K_{dp}(s) \gamma_{hh,dp}^{(R_c)}(s) ds}{\int_{r_0}^r K_{dp}(s) ds} \quad (3)$$

where $\gamma_{hh,dp}^{(R_c)}(r)$ is the value of $\gamma_{hh,dp}$ corresponding to the hydrometeor class R_c detected at the range distance r . The proposed methodology has shown promising adaptive capability to the raindrop size distribution variability when compared with other approaches, on one hand, and the need to deal with potential ice contamination, on the other hand.

As a matter of fact, wet hail can produce huge co-polar attenuation and, depending on the size, differential attenuation. According to the melting model of hail proposed by Rasmussen and Heymsfield (1987), small hail (diameters less than 10-12 mm) assumes an oblate shape (Z_{dr} and α_{dp} positive) during melting, while greater hailstones are subject to shedding that confers them an almost isotropic appearance (Z_{dr} and α_{dp} approximately null). Moreover, due to resonance scattering effects at C band, melting hailstones in the diameter range 6-8 mm cause the enhancement of differential reflectivity with respect to a fully melted particle of the same axis ratio (Bringi and Chandrasekar, 2001).

2.2 IMPROVED APDP APPROACH

In order tackle the above mentioned observations, an improved version of APDP has been developed by implementing a preliminary full hydrometeor

classification. The general block diagram of the improved APDP algorithm is shown in Figure 1. Regarding the hydrometeor classification algorithm, a fuzzy-logic based approach, adapted from Marzano et al. (2007), has been preferred to the model-supervised Bayesian scheme considering it more suitable for an empirical tuning as needed for operational purposes.

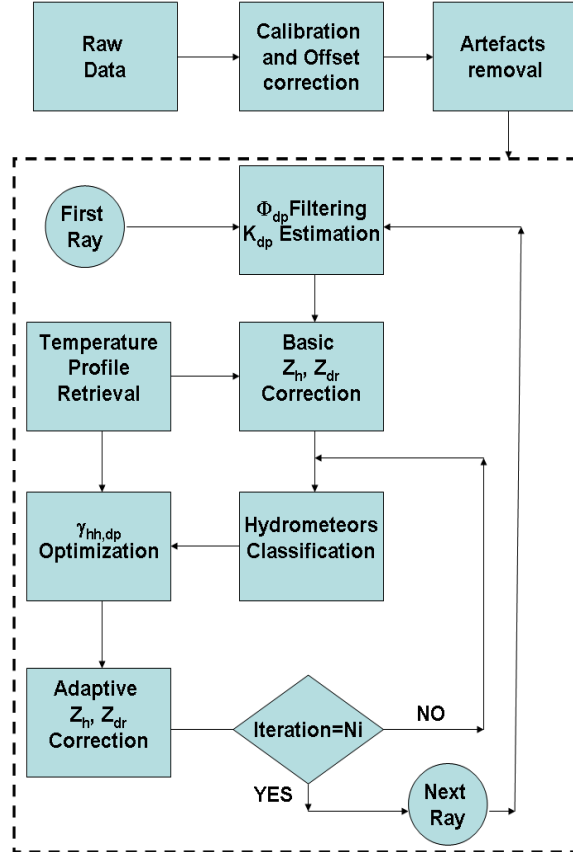


Figure 1. Block diagram of the proposed attenuation correction scheme with embedded hydrometeors classification.

According to scattering simulations performed in this work, the fundamental hypothesis behind the proposed methodology is that the linear relationship between $\alpha_{hh,dp}$ and K_{dp} is still approximately valid either for horizontally oriented wet hail or for rain/hail mixture. It is worth mentioning that tumbling hail does not contribute significantly to differential phase shift, while vertically oriented hail produces negative K_{dp} . The resulting effect is that relationships employing Z_{hh} and Z_{vv} such as

$$\alpha_{hh} = a_h Z_{hh}^{b_h} \quad (4)$$

$$\alpha_{vv} = a_v Z_{vv}^{b_v} \quad (5)$$

must be used in place of (1)-(2) for attenuation estimation and correction. The main issue of using (4)-(5) is the calibration error dependency.

Because, the adopted hydrometeor classification algorithm does not attempt to discriminate between the

different hail fall modes, an *a posteriori* analysis based on the corrected Z_{dr} and K_{dp} is required to infer the hail orientation. In other words, given that hail has been identified, null, negative or positive Z_{dr} and K_{dp} are attributed to tumbling, vertically or horizontally oriented hail, respectively. According to the inferred orientation, the suited specific attenuation estimator is chosen among (1)-(5).

3. CASE STUDY AND EXPERIMENTAL RESULTS

As shown in the block diagram of Figure 1, the attenuation correction procedure with the embedded hydrometeor classification follows a robust data quality check that is routinely applied in order to mitigate radar miscalibration, radome interference, system offsets (Gourley et al. 2006a) and artefacts (i.e., ground clutter, anaprop, insects, birds).

Data collected at vertical incidence (one scan each 15 minutes) are used to estimate the calibration error on Z_{dr} according to the procedure proposed by Gorgucci et al. (1999). Absolute calibration error estimate is performed by means of the self-consistency principle (Gourley et al. 2006b). In order to compensate for system noise and Mie scattering effects, an iterative Finite Impulse Response (FIR) filter is applied to the measured differential phase (Hubbert and Bringi 1995) using a moving window of about 3 km.

3.1 CASE STUDY

The extreme convective event occurred on 23 June 2005 in the Paris area has been considered in the present work.

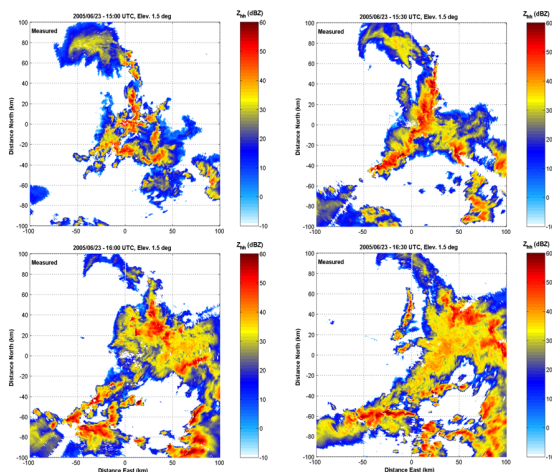


Figure 2. Time evolution of reflectivity fields during the convective event observed on 23 June 2005.

This unusual event was characterized by path integrated attenuation up to about 20 dB. The path

integrated differential attenuation (PIDA) was even larger than 10 dB as demonstrated by the saturated low (about -10 dB) measured values of Z_{dr} (in dB). In order to reduce ground clutter contamination and the influence of the melting layer on the evaluation of the attenuation correction methods, only the 1.5 degrees antenna elevation scans were considered.

Figure 2 shows the time evolution of the observed reflectivity field with a time step of 30 minutes starting at 1500 UTC and ending at 1630 UTC. Very intense convective cells, characterized by Z_{hh} and Z_{dr} peaks above 60 dBZ and 6 dB, respectively, occurred during the whole event. Furthermore, a huge differential phase shift often larger than 200 degrees with peaks above 250 degrees was observed around 1530 UTC.

3.2 EXPERIMENTAL RESULTS

Both the observed reflectivity and differential reflectivity PPIs at 15:25 UTC (upper panels) and the corrected (middle panels) are shown in Figure 3. In the same figure, the lower left and right panels show the correlation coefficient and the corresponding hydrometeor types, respectively.

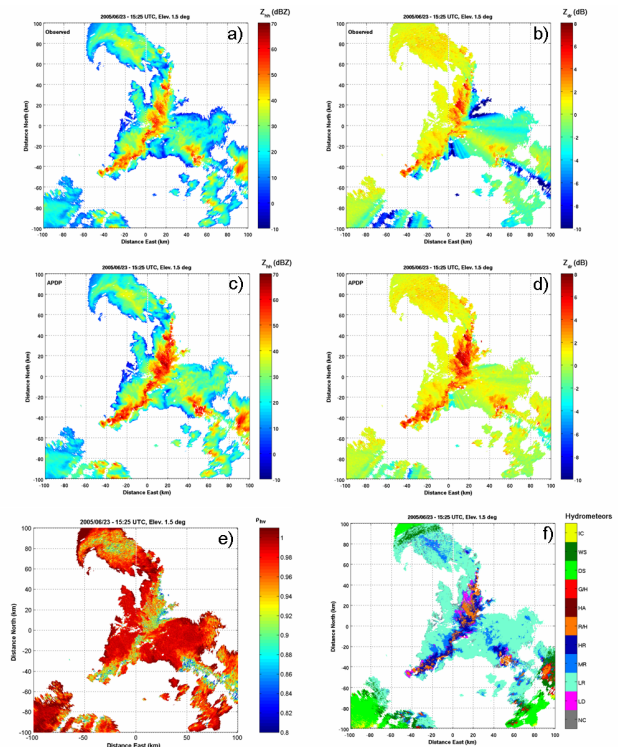


Figure 3. PPIs of polarimetric radar variables and the corresponding hydrometeor types (Fig. 3 f). Figures 3 a-d) show the observed (a,b) and corrected (c,d) Z_{hh} , Z_{dr} , respectively. Figure 3 e) shows the correlation coefficient.

The effects of strong attenuation causes a significant azimuthal heterogeneity of the Z_{dr} fields as it is evident

by the largely negative area shown in Figure 3b. After the correction procedure is applied, the reflectivity and differential reflectivity fields are almost completely recovered (see Figures 3 c-d)).

According to the low values of the correlation coefficient ($\rho_{hv} < 0.9$), the attenuating cells were mainly characterized by the presence of heavy rain, large drops and rain/hail mixture (see Figure 3f)).

Figure 4 indicates that in azimuthal sector comprised between 35 and 75 degrees the differential phase shift is larger than 100 degrees with peaks above 250 degrees (see 3rd panel of Figure 4). In that area (see 2nd panel of Figure 4) the observed Z_{dr} drops down to -10 dB (lower threshold value), the occurrences of identified hydrometeors showing the large presence of rain/hail mixture.

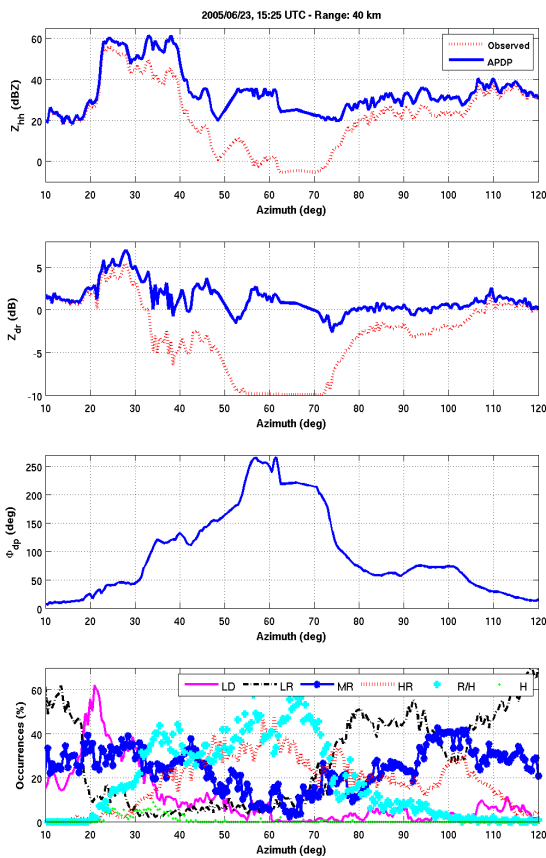


Figure 4. Plot of observed and corrected Z_{nh} (upper panel) and Z_{dr} (middle panel) as a function of the azimuth (between 10 and 120 degrees) for a fixed range distance (40 km) relatively to the event of June 23rd 2005 at 15:25 UTC. The third and fourth panels show the corresponding plots of ϕ_{dp} and identified hydrometeor classes (i.e, Large Drops LD, Light Rain LR, Moderate rain MR, Heavy Rain HR, Rain/Hail R/H, Hail H), respectively.

4. CONCLUSIONS

An adaptive method for attenuation correction based on the use of differential phase with an embedded Fuzzy-Logic hydrometeor classification has been applied to an extreme convective event observed in the Paris area on 23 June 2005. The detected presence of rain/hail mixture has been evaluated as the main cause of the huge observed co-polar attenuation and differential attenuation. The application of the proposed methodology has shown a remarkable performance in reducing the heterogeneity of the observed reflectivity and differential reflectivity fields.

Future efforts will be devoted to the comparison of the results obtained by applying the proposed hail detection methodology with in situ observations.

5. REFERENCES

Alberoni, P.P., D.S. Zrnić, A.V. Ryzhkov and L. Guerrieri, 2002: Use of a fuzzy logic classification scheme with a C-band polarimetric radar: first results. Proc. of ERAD02, 324-327.

Bringi, V. N., T. A. Seliga, and K. Aydin, 1984: Hail detection with a differential reflectivity radar. Science, 225, 1145-1157.

Bringi, V. N., V. Chandrasekar, N. Balakrishnan, and D. S. Zrnić, 1990: An examination of propagation effects in rainfall on radar measurements at microwave frequencies. J. Atmos. Ocean. Technol., 7, 829-840.

Cook, B., 1958: Hail determination by radar analysis. Mon. Wea. Rev., 86, 435-438.

Gorgucci, E., G. Scarchilli, and V. Chandrasekar, 1999: A procedure to calibrate multiparameter weather radar using properties of the rain medium. IEEE Trans. Geosci. Rem. Sens., 37, 269-276.

Gourley, J. J., P. Tabary, J. Parent-Du-Chatelet, 2006a: Data quality of the Meteo-France C-band polarimetric radar. J. Appl. Meteor., 33, 1340-1356.

Gourley, J. J., P. Tabary, J. Parent-Du-Chatelet, and A. Illingworth, 2006b: Radar calibration using consistency of polarimetric parameters and constraints for drop shapes. Proceed. of 4th European Radar Conf., Barcelona, 18-22 September.

Heinselman, P. L., and A. V. Ryzhkov, 2006: Validation of polarimetric hail detection. Wea. Forecasting, 21, 839-850.

Jameson, A.R., 1992: The effect of temperature on attenuation-correction schemes in rain using polarization propagation differential phase shift. J. Appl. Meteor., 31, 1106-1118.

Knight, C. A., and N. C. Knight, 1970: The falling behaviour of hailstones. *J. Atmos. Sci.*, 7, 672-681.

Marzano, F. S., D. Scaranari, and G. Vulpiani, 2007: Supervised fuzzy-logic classification of hydrometeors using C-band weather radars. *IEEE Trans. Geosci. Rem. Sensing*, in press.

Meischner, P. F., V. N. Bringi, D. Heimann, and H. Holler, 1991: A squall line in southern Germany: kinematics and precipitation formation as deduced by advanced polarimetric and Doppler radar measurements. *Mon. Wea. Rev.*, 119, 678-701.

Rasmussen, R. M., and A. J. Heymsfield, 1987: Melting and shedding of graupel and hail. Part I: Model Physics. *J. Atmos. Sci.*, 44, 2754-2763.

Smyth, T. J., T. M. Blackman, and A. J. Illingworth, 1999: Observations of oblate hail using dual polarization radar and implications for hail-detection schemes, *Q. J. R., Meteorol. Soc.*, 125, 993-1016.

Testud, J., E. Le Bouar, E. Obligis, and M. Ali-Mehenni, 2000: The Rain Profiling Algorithm Applied to Polarimetric Weather Radar. *J. Atmos. Oceanic Technol.*, 17, 332-356.

Vivekanandan, J., D.S. Zrnić, S.M. Ellis, R. Oye, A.V. Ryzhkov, and J. Straka, 1999: Cloud microphysics retrieval using S-band dual-polarization radar measurements. *Bulletin of the American Meteor. Soc.*, 80, 381-388.

Vulpiani, G., F. S. Marzano, V. Chandrasekar and S. Lim, 2005: Constrained iterative technique with embedded neural-network for dual-polarization radar correction of rain path attenuation. *IEEE Trans. Geosci. Rem. Sensing*, 43, 2305-2314.

Vulpiani, G., P. Tabary, J. Parent-Du-Chatelet, and F. S. Marzano, 2006: Comparison of advanced radar polarimetric techniques for operational attenuation correction at C Band. Submitted to *J. Atmos. Oceanic Technol.*

Waldvogel, A., B. Federer, and P. Grimm, 1979: Criteria for the detection of hail cells. *J. Appl. Meteor.*, 18, 167-172.

Zrnić, D. S., A. V. Ryzhkov, J. Straka, Y. Liu, and J. Vivekanandan, 2001: Testing a procedure for the automatic classification of hydrometeor types. *J. Atmos. Oceanic Technol.*, 18, 892-913.